Available online at www.sciencedirect.com
SCIENCE DIRECT®
Physica C 412–414 (2004) 864–870
PHYSICA C
www.elsevier.com/locate/physc

Improvement of in-plane alignment for surface oxidized NiO layer on textured Ni substrate by two-step heat-treatment

Katsuya Hasegawa [a,*], Toru Izumi [a], Teruo Izumi [a], Yuh Shiohara [a], Toshihiko Maeda [b]

[a] *Superconductivity Research Laboratory, International Superconductivity Technology Center, 1-10-13 Shinonome, Koto-ku, Tokyo, 135-0062 Japan*
[b] *The Furukawa Electric Co., Ltd., Nikko 321-1493, Japan*

Received 29 October 2003; accepted 13 January 2004
Available online 7 May 2004

Abstract

Epitaxial growth of NiO on a textured Ni substrate as a template for an $REBa_2Cu_3O_y$ coated conductor was investigated. Highly in-plane aligned NiO layers were successfully fabricated using a new process of a two-step heat-treatment for oxidation. In the first-step, a highly in-plane aligned thin NiO layer was formed on a textured Ni substrate under a low driving force of oxidation. Then, in the second-step, a thick NiO layer was grown at a higher rate with maintaining its high in-plane grain alignment, as if the first NiO layer acts as a seed crystal layer. Further, growth rates and microstructures of the NiO layers were studied comparatively in the cases with and without the first layer. It was found that the oxidation rate in the case with the first layer was lower than that without the first layer. The microstructure observation revealed that the NiO without the first layer was poly-crystalline with many grain-boundaries. On the other hand, in the case with the first layer, grain-boundaries of the NiO were hardly observed. Hence, the reason for this difference of the growth rate and the microstructure of the NiO layers were discussed in view of a diffusivity path.

PACS: 74.72.Bk; 74.76.Bz
Keywords: Surface oxidation; NiO; In-plane crystal alignment

1. Introduction

In-plane grain crystal alignments of RE-$Ba_2Cu_3O_y$ (RE123: RE = Y, Sm, Nd...) on metal substrates for coated conductors are introduced by textured buffer layers or substrates. A surface oxidized NiO layer on a textured Ni by the so-called SOE (surface oxidation epitaxy) method is one of the promising candidates because of its simple process which is suitable for low-cost fabrication [1]. However, deterioration of the in-plane alignment of the NiO layer was inevitable, i.e., in-plane FWHM (full width at half maximum) values evaluated from ϕ-scan measurement of X-ray diffraction (XRD) for the NiO layers were worse than those of the textured Ni substrate. Indeed, the

* Corresponding author. Tel.: +81-3-3536-5711; fax: +81-3-3536-5714.
E-mail address: khasegawa@istec.or.jp (K. Hasegawa).

0921-4534/$ - see front matter © 2004 Elsevier B.V. All rights reserved.
doi:10.1016/j.physc.2004.01.106

deterioration of the NiO prepared by the conventional SOE (cSOE) method was confirmed in our previous study [2]. In consequence, degrees of in-plane grain alignment of thereon $BaZrO_3$ (BZO) buffer and $SmBa_2Cu_3O_y$ (Sm123) films were limited, whose in-plane FWHM values ranged between 12° and 28° which are too large to realize higher J_c values than 1×10^6 A/cm^2.

In this study, improvement of in-plane grain alignment for the surface oxidized NiO layer as a template of an RE123 coated conductor was investigated. A highly in-plane aligned NiO layer was realized by this modified SOE process (mSOE). Applicability of the newly developed, mSOE-grown NiO layer was confirmed by high-J_c Sm123 coated conductors [3].

2. Experimental

Specimens were cut from a {1 0 0} ⟨0 0 1⟩ cube-textured Ni tape of 10 mm in width and 70 μm in thickness. The textured Ni substrate was confirmed to be highly out-of-plane and in-plane aligned from an XRD measurement, which shows in-plane FWHM values about 7° in ϕ-scan of Ni(1 1 1) and a strong (2 0 0) peak and no other diffractions in the θ–2θ profiles. A heat-treatment for oxidation was conducted under the following conditions: temperature was ranged from 750 to 1200 °C, time from 10 min to 5 h, Oxygen partial pressure ($P(O_2)$) from 5×10^{-3} to 2×10^4 Pa. Crystal orientation was characterized by XRD and the pole-figure measurements. Its surface roughness was measured by using a stylus profiler with a scan-length of 500 μm. Thicknesses of the NiO layer were measured directly from the cross-sectional optical microscopy and scanning electron microscopy (SEM) images. Further, the grain structure of the NiO layer was investigated after electrolytically etching with CH_3COOH and HF in H_2O to distinguish grain-boundaries [4].

3. Results and discussion

So far, growth conditions of SOE-NiO were reported from several groups [5]. Almost all of them employed the conditions of high-temperatures over 1000 °C and high $P(O_2)$ near the ambient pressure, as a heat-treatment for oxidation. Those conditions have an advantage of relatively higher growth rates than 1 μm/min [5,6]. In view of crystal growth, however, a higher growth rate due to higher supersaturation occasionally induces a lower crystallinity such as unfavorable oriented or non-epitaxial nucleation. In the SOE-NiO growth, the supersaturation ratio (σ) could be defined as,

$$\sigma = P(O_2)/P(O_2)^* \quad (1)$$

where $P(O_2)^*$ is the equilibrium pressure of O_2 at a certain temperature. $P(O_2)^*$ values for the NiO/Ni system calculated from thermodynamical data [7] were as low as 10^{-10} Pa at 750 °C. Therefore, oxidation of Ni may proceed under the much lower $P(O_2)$ atmosphere than the above-mentioned conditions.

Fig. 1 shows $P(O_2)$ dependences of in-plane FWHM, degree of (1 0 0) orientation, and the surface roughness. The $P(O_2)$ was ranged from 5×10^{-3} to 50 Pa using a tube furnace under an O_2/Ar mixture gas flow with vacuum pumping. The annealing temperature and the time were employed as following two conditions: (a) 750 °C × 10 h, (b) 1100 °C × 1 h. All the data except for 1100 °C and $P(O_2)$ of 50 Pa show the same tendency that the in-plane alignment was improved as the $P(O_2)$ decreased, accompanying both the higher degrees of (1 0 0) orientation and a lower average surface roughness (R_a). In-plane FWHM values were reached about 7° in the low $P(O_2)$ conditions in this study, which is close to that of the Ni substrate.

Not only in-plane alignment but also out-of-plane alignment of NiO was improved by maintaining the low $P(O_2)$ atmosphere. Fig. 2 shows XRD θ–2θ profiles of the Ni substrate and thereon NiO: (a) Ni substrate, (b) mSOE-NiO (after the first-step heat-treatment), (c) mSOE-NiO (after the second-step one), (d) cSOE-NiO. It should be noted that the vertical axis is a logarithmic scale. The second-step heat-treatment was 1200 °C × 2 h in air, and the same heat-treatment was conducted for cSOE-NiO growth as shown in Fig. 2(d). It was clearly observed that the NiO layer grown by the

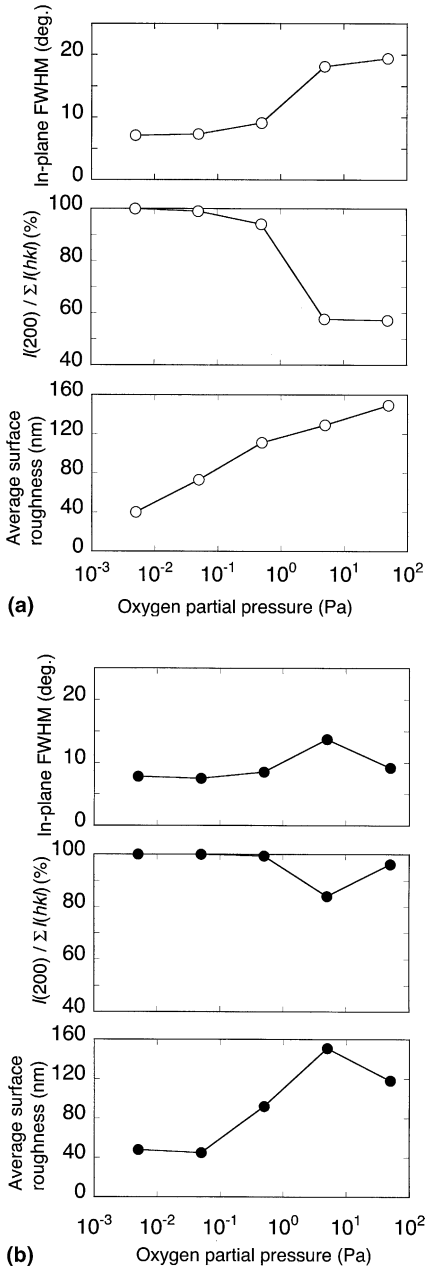

Fig. 1. Oxygen partial-pressure dependence of in-plane FWHM, degree of (1 0 0) orientation, and surface roughness. Annealing temperature and time were as follows: (a) 750 °C× 10 h, (b) 1100 °C×1 h.

cSOE method shows several diffractions other than (2 0 0) plane. The index of the (1 0 0) orientation fraction defined as $I(200)/\sum I(hkl)$ was

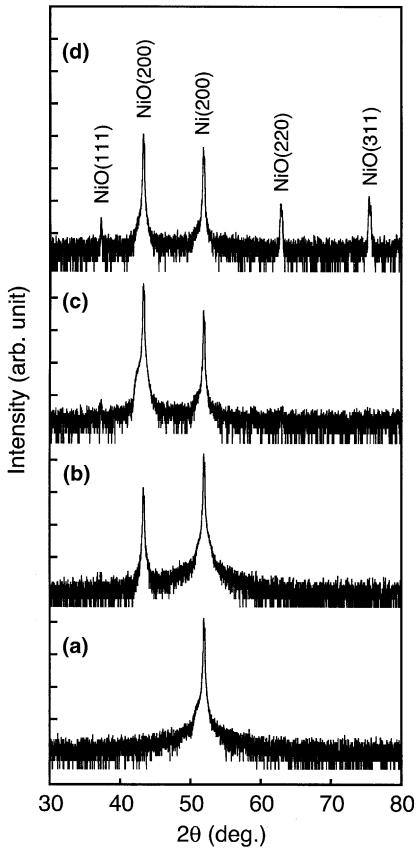

Fig. 2. XRD θ–2θ profiles of Ni substrate and SOE-grown NiO: (a) Ni substrate, (b) modified SOE (after the first-step), (c) modified SOE (after the second-step), (d) conventional SOE. Note that the vertical axis was a logarithmic scale.

about 98%. In contrast, the NiO layer grown by the mSOE method shows only (2 0 0) diffraction. After the second-step of mSOE, intensities of NiO(2 0 0) became stronger than those after the first-step because of the increased NiO thickness.

XRD pole figures of the SOE-grown NiO(1 1 1) were summarized in Fig. 3: (a) mSOE (after the first-step), (b) mSOE (after the second-step), (c) cSOE. The mSOE-NiO, both after the first-step and after the second-step, showed a four-fold symmetry with sharp peaks. The cSOE-NiO also showed a four-fold symmetry, but their peaks were much broader than those of mSOE-NiO.

Fig. 4 shows thickness dependences of in-plane FWHM of NiO(1 1 1); solid symbols represent the

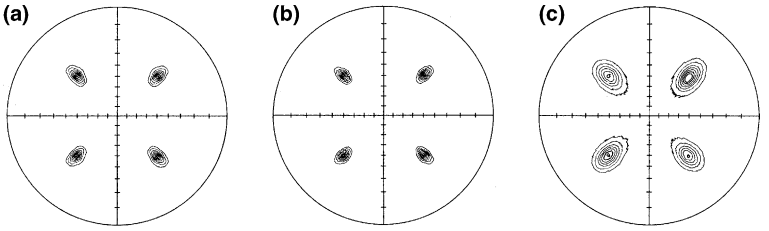

Fig. 3. XRD pole figures of SOE-grown NiO(1 1 1): (a) modified SOE (after the first-step), (b) modified SOE (after the second-step), (c) conventional SOE. In-plane FWHM values were 7.2°, 7.5°, and 14.0°, respectively.

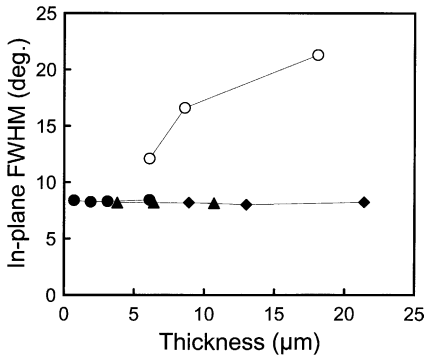

Fig. 4. Thickness dependence of in-plane FWHM of NiO(1 1 1); solid symbols represent the mSOE-grown NiO layers and open symbols for the cSOE-grown NiO layers. (●) mSOE at 1000 °C, (▲) mSOE at 1100 °C, (◆) mSOE at 1200 °C, (○) cSOE at 1000 °C.

mSOE-grown NiO layers and open symbols for the cSOE-grown NiO layers. Significant difference between mSOE and cSOE was observed in the trends of the relationship between in-plane grain alignment and its thickness. That is, lower in-plane FWHM values with almost completely flat trends were recognized at any annealing temperatures and growth thicknesses in the case of mSOE-NiO. On the other hand, in the case of cSOE-NiO, in-plane FWHM values were worse than those of mSOE-NiO and increased with increasing its thickness.

Fig. 5 shows thicknesses of the SOE-grown NiO layers as a function of the annealing time: (a) cSOE and (b) mSOE method. For the case of mSOE, the annealing time was those of the second-step. All data of the NiO thickness (x) and the time for oxidation (t) was fitted to the well-known parabolic growth equation, which is defined as a solution of the differential equation $dx/dt = 2k_p/t$,

$$x^2 = k_p t + c \tag{2}$$

where k_p is a so-called parabolic rate-constant and c is an integration constant. The physical meaning of k_p was explained by Wagner [8] where the material

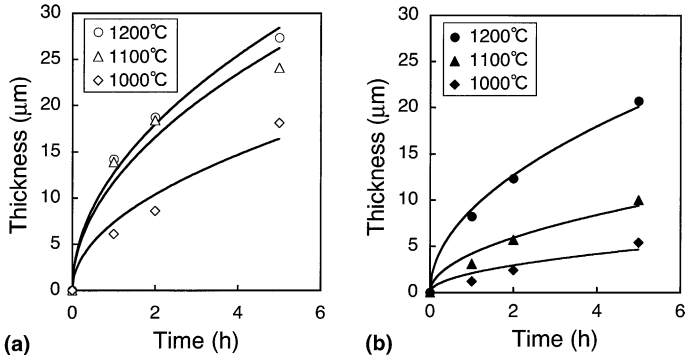

Fig. 5. Thicknesses of the SOE-grown NiO layer as a function of the annealing time: (a) conventional SOE, (b) modified SOE. The growth rate of the NiO by the modified SOE was always lower than that of the conventional SOE method as compared at the same annealing temperature.

is transported by diffusion across a single and homogeneous layer of the reaction product. The constant, c, is estimated by the boundary condition of the thickness x at $t = 0$. In the case of cSOE, $c = 0$ was obtained, since oxidation started form a bare-Ni surface. While in the case of mSOE, $c = 0.7$ μm, which is the thickness of the NiO layer by the first-step annealing, was employed. The values of k_p were calculated by a least-squares approximation method. Then, $x - t$ curves using the obtained k_p values at different annealing temperatures were also plotted in Fig. 5. The k_p, and hence, the growth rate of the NiO layer by mSOE was always lower than that of the cSOE method when compared at the same annealing temperature.

Fig. 6 shows the Arrhenius plot for k_p of the SOE-grown NiO layers at the temperature range from 1000 to 1200 °C. The broken-line shows the experimental results of single-crystalline NiO/Ni by Graham et al. [9]. In the case of mSOE-NiO, the k_p and the activation energy were both close to those of Graham et al. While, in the case of cSOE-NiO, the k_p values were larger and the activation energy was smaller than the others. The calculated $k_{p,l}$ value by Rhines and Connell [10] using a volume diffusion coefficient, D_l, of Ni in NiO was also plotted for comparison. The reason for the different growth rates between mSOE and cSOE is discussed at the later part of this section.

Fig. 7 shows surface optical microscopy images of the NiO layers grown by (a) cSOE and (b) mSOE methods. The surfaces of the NiO layers were mechanically polished and etched electrolytically to distinguish grain-boundaries. It can be found that the NiO layer without the first layer

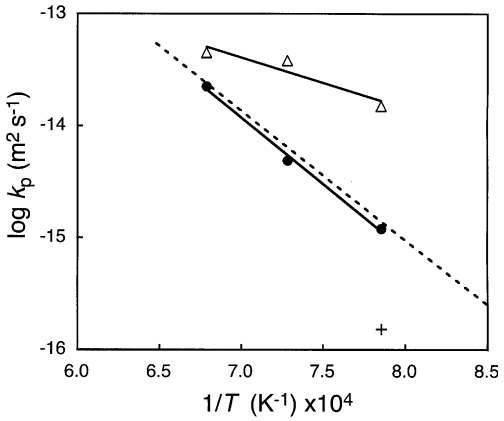

Fig. 6. Arrhenius plot for parabolic rate-constant (k_p) of NiO layers grown by mSOE (●) and cSOE (△). Temperature ranged from 1000 to 1200 °C. The values of k_p were obtained by a least-squares method from data of Fig. 5. Broken-line shows the experimental results of single-crystalline NiO/Ni [9]. (+): calculated $k_{p,l}$ value by Rhines [10] using the volume diffusion coefficient, D_l, for Ni in NiO was also plotted for comparison.

consists of poly-crystalline grains with many grain-boundaries. On the other hand, in the case of mSOE, grain-boundaries of the NiO were hardly observed even after electrolytical etching. Considering the facts that the underlying Ni substrate consists of relatively large grains whose grain-boundaries were clearly observed by optical microscopy and that in-plane FWHM values of mSOE-NiO were the same as the Ni substrate, mSOE-NiO may also have grain-boundaries due to misorientation angles between grains, even though the degree of epitaxy of the NiO on Ni was ideally proceeded. Possible explanations for this observation of few grain-boundaries in

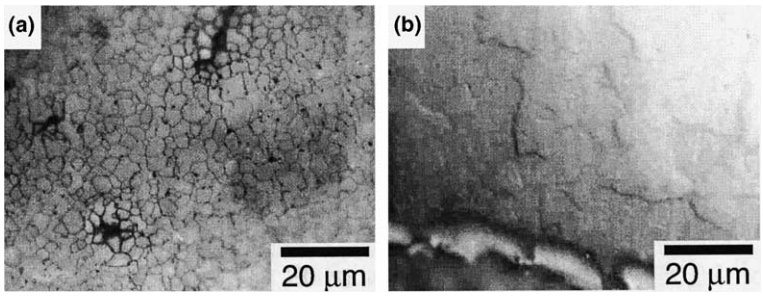

Fig. 7. Surface optical microscopy images of NiO layer grown by (a) conventional SOE, (b) modified SOE. The surfaces of the NiO layer were polished mechanically and etched electrolytically to distinguish grain-boundaries.

Table 1
Comparison of density of grain-boundary, k_p and apparent diffusivity for the NiO layers grown by cSOE and mSOE methods

Method	Density of grain-boundary (m^{-1})	Density of dislocation-pipe (m^{-2})	$k_p/k_{p,l}$ (1000 °C)	D_{app}/D_l
cSOE	4.7×10^5	2.0×10^{14}	99	390
mSOE	4.4×10^4	1.1×10^{13}	7.9	23

Density of grain-boundary was evaluated from surface optical microscopy images and the ratio of k_p values were from the data in Fig. 6. The contribution of grain-boundaries to the apparent diffusivity was estimated based on the Hart's model [12].

mSOE-NiO are as follows: If the mSOE-NiO consists of continuous domains though small-angle grain boundary are connected strongly each other, the grain-boundaries are hardly etched similarly to the single crystals of NiO.

Finally, the above-mentioned different k_p values and microstructures between mSOE and cSOE methods were reasonably explained by grain-boundary diffusions. The apparent diffusivity of Ni in NiO, D_{Ni}, was measured through the oxidation study of Ni by Fueki and Wagner [11]. In their proposed model, the value of D_{Ni} was evaluated experimentally using $P(O_2)$ dependences of k_p. In this study, the k_p values were obtained only at the fixed $P(O_2)$ of 2×10^4 Pa. However, Fueki's data show that D_{Ni} is proportional to the k_p values, at least in the heat-treatment conditions employed in this study. Then, in the followings, we assume the ratio of k_p was the same as that of the ratio of D_{Ni}. The contribution of grain-boundaries was estimated based on the Hart's model [12], in which grain-boundaries consist of "dislocation-pipes" with the specific distance derived from misoriented angles. Detailed treatments for a high-diffusivity path of the NiO will be described elsewhere [13]. Here the experimental data and theoretical values were summarized in Table 1. The tendency of the experimental data coincide well with the theoretical value of the Hart's model. Thus, the reason for the difference in the oxidation-rates was correlated to microstructures at least qualitatively.

4. Conclusion

A new process of the two-step heat-treatment for surface oxidation of textured Ni substrates was developed. In the first-step, a highly in-plane aligned thin NiO layer was formed on the textured Ni substrate under the low driving force of oxidation. Then, in the second-step, a highly in-plane aligned thick NiO layer was grown at higher rates. In addition, it was revealed that the modified SOE-grown NiO layer shows a single-crystalline microstructure, which is much different from that of the conventional SOE-grown NiO layer. Further, the correlation between the oxidation rate and the microstructure was explained in view of grain-boundary diffusion at least qualitatively.

Acknowledgements

This work was supported by the New Energy and Industrial Technology Development Organization (NEDO) as Collaborative Research and Development of Fundamental Technologies for Superconductivity Application.

References

[1] K. Matsumoto, Y. Niiori, I. Hirabayashi, N. Koshizuka, T. Watanabe, Y. Tanaka, M. Ikeda, in: K. Osamura, I. Hirabayashi (Eds.), Advances in Superconductivity, vol. 10, Springer-Verlag, Tokyo, 1998, pp. 611–614.
[2] M. Kai, N. Hobara, K. Hasegawa, T. Izumi, S. Asada, Y. Nakamura, T. Izumi, T. Watanabe, Y. Shiohara, Physica C 378–381 (2002) 998.
[3] T. Izumi, K. Hasegawa, S. Asada, T. Izumi, Y. Shiohara, T. Maeda, paper in preparation.
[4] F.N. Rhines, R.G. Connell Jr., M.S. Choi, J. Electorochem. Soc.: Solid-State Sci. Technol. 126 (1979) 1061.
[5] Z. Lockman, A. Berenov, W. Goldacker, R. Nast, B. deBoer, B. Holzapfel, J.L. MacManus-Driscoll, J. Mater. Res. 18 (2003) 327.
[6] K. Matsumoto, T. Watanabe, T. Tanigawa, T. Maeda, S.B. Kim, I. Hirabayashi, IEEE Trans. Appl. Supercond. 11 (2001) 3138.
[7] O. Kubaschewski, C.B. Alcock, Metallurgical Thermochemistry, fifth ed., revised and enlarged, Pergamon Press, 1979, p. 382.

[8] C. Wagner, Z. Physik. Chem. 21B (1933) 25.
[9] M.J. Graham, D. Caplan, M. Cohen, J. Electorochem. Soc.: Solid-State Sci. Technol. 119 (1972) 1265.
[10] F.N. Rhines, R.G. Connell Jr. Stress effects and the oxidation of metals. in: Proceedings of the Symposium held at the 1974 TMS-AIME fall meeting, Metallurgical Society of AIME, 1975, pp. 94–113.
[11] K. Fueki, J.B. Wagner Jr., J. Electorochem. Soc.: Solid-State Sci. Technol. 112 (1965) 384.
[12] E. Hart, Acta Met. 5 (1957) 597.
[13] K. Hasegawa et al., paper in preparation.